

## Ambient Earth noise: A survey of the Global Seismographic Network

Jonathan Berger and Peter Davis

Institute of Geophysics and Planetary Physics, Scripps Institution of Oceanography, University of California San Diego, La Jolla, California, USA

Göran Ekström

Department of Earth and Planetary Sciences, Harvard University, Cambridge, Massachusetts, USA

Received 25 August 2004; revised 15 September 2004; accepted 20 September 2004; published 16 November 2004.

[1] It has been a decade since the last comprehensive model of ambient Earth noise was published (Peterson, 1993). Since then, observations of ambient Earth noise from the Incorporated Research Institutions for Seismology (IRIS) Global Seismographic Network (GSN) of widely distributed, similarly equipped, and well-calibrated stations have become available. The broad geographic sampling of this large data set and the ease of access to waveform data provided by the IRIS Data Management System facilitate analysis of global noise samples. We have analyzed data from the 118 GSN stations operating during the year July 2001 through June 2002. On the basis of over 738,000 hourly spectral estimates computed from these stations' data, we have developed a robust noise model that exhibits significant differences from previous models both in the normal mode and body wave bands. Our analysis technique has the advantage that we do not need to search for quiet periods but can include all data where the instruments are operating correctly. *INDEX TERMS:* 7299 Seismology: General or miscellaneous; 7294 Seismology: Instruments and techniques; 7255 Seismology: Surface waves and free oscillations; *KEYWORDS:* ambient Earth noise, Global Seismographic Network

**Citation:** Berger, J., P. Davis, and G. Ekström (2004), Ambient Earth noise: A survey of the Global Seismographic Network, *J. Geophys. Res.*, 109, B11307, doi:10.1029/2004JB003408.

### 1. Introduction

[2] After 20 years of operation, the Incorporated Research Institutions for Seismology (IRIS) Global Seismographic Network (GSN) [Butler *et al.*, 2004] has produced a vast amount of high-quality, digital data collected from widely distributed, similarly equipped and well-calibrated stations. These data, in addition to being used to improve our knowledge of earthquakes and the structure of the Earth's interior, provide information on the Earth's ambient seismic noise. A global model of seismic background noise can be used to set requirements for the sensors and data acquisition systems of the next generation of GSN instrumentation, a process now underway.

[3] The seismic noise model most commonly referenced today [Peterson, 1993] is over 10 years old and was based on data recorded at a variety of stations during periods of apparent low seismic noise. In this paper, we develop a new model based on recordings from the entire GSN made over a 1 year period. The total amount of data processed (over 1 Terabyte) and the computation capabilities of the data processing center hardware (with many CPUs faster than 1 GHz) vastly exceed what was available when the Peterson study was conducted. By evaluating the noise level at many geographically distributed collection points over a period of

time long enough to include seasonal variation, we hope to gain a better understanding of the global levels of seismic noise. Further, because instrumentation of the GSN stations is far more uniform than in the stations used in the original study, we will reduce the effects that variations in hardware might introduce into the data set.

[4] Several early studies [Brune and Oliver, 1959; Frantii *et al.*, 1962; Fix, 1972; Murphy and Savino, 1975; Agnew and Berger, 1978; Peterson, 1980] showed the main features of the Earth's ambient noise spectrum: the microseism peaks at 4–6 and 15 s, a minimum at around 30 s, and the general increase at longer periods. Peterson [1993] marked the first comprehensive global study from a variety of networks then in operation. IRIS sponsored a study of the noise at its stations that was reported in the FDSN Station Book [Incorporated Research Institutions for Seismology, 1994]. All of these studies relied on careful selection of data segments to avoid "contamination" by earthquake signals, and various spectral averaging techniques were employed. Peterson's [1993] model (hereinafter called the PLNM) consisted of 21 straight line segments fit to the envelope of the minima of the individual spectra in a log-log plot.

[5] Data recorded at the IRIS Global Seismographic Network (GSN) forms the basis of this study. The network's chief features are (1) standardized equipment specifications (all stations are instrumented to meet uniform requirements of high dynamic range, wide bandwidth and accurate timing); (2) centralized operations and maintenance (the

## Global Seismograph Network

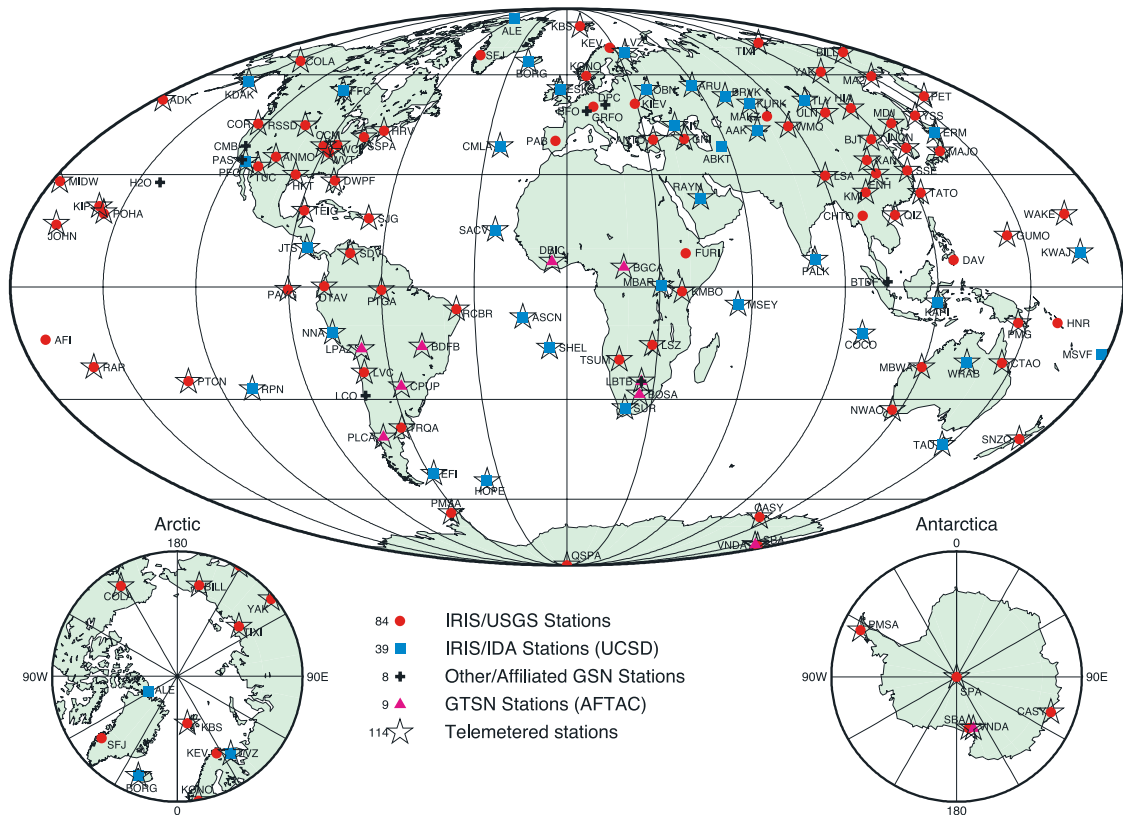


**Figure 1.** Map of the 118 Global Seismograph Network (GSN) stations that produced data used in this study.

network is operated and maintained to common performance standards; data quality is routinely reviewed and station performance assessed to evaluate how well these standards are being met (the authors are responsible for the operation and maintenance of a portion of the IRIS GSN and for monitoring the quality of the data collected); (3) common data format (all data are archived and distributed in SEED [Ahern *et al.*, 1994], the common exchange format of the Federation of Digital Seismic Networks (FDSN)); (4) freely accessible data archive (the data used in this study are freely available to the research public through the IRIS Data Management System).

[6] When we began this study in early 2003, we judged that the IRIS DMC archives were complete up to a date 6 months earlier. That is, not all data from the latter half of 2002 had arrived in the network operators' data collection centers and been forwarded to the IRIS DMC. Therefore we chose to analyze data recorded at the 118 stations of the GSN that were operating during the 1 year period, July 2001 to June 2002. A 1 year observing period is long enough to capture the effects of seasonal variation, which can be quite large at some stations. Figure 1 shows a map of the stations utilized. The geographic distribution of the stations includes a broad sampling of both continental and oceanographic sites as well as climate zones from the tropics to the polar regions.

[7] The GSN sensors include (1) three-component broadband seismometers, either a KS54000 or KS36000 installed

in a borehole, or an STS-1VBB installed in a vault, with data recorded at continuously 20 samples per second (sps); (2) about half of the stations are equipped with auxiliary sensors, either GS13, S13, STS-2 or CMG3T, with data recorded continuously, usually at 40 sps; (3) many stations are also equipped with strong motion accelerometers, usually an FBA-23, continuously recorded at 1 sps and triggered recordings at 100 sps although these channels were not used in this study; (4) some stations are equipped with pressure sensors recording the local barometric pressure at 1.0 or 0.5 sps.

[8] The locations of the GSN stations are chosen to minimize man-made and environmental noise insofar as practical. The instruments are designed and installed to record accurately the local ambient Earth motion. Each acquisition system is thoroughly tested before deployment to verify that system performance meets specifications. Extreme care is taken to place each seismometer in a well insulated environment and as free of stray electromagnetic fields as possible. The very broadband sensors are either installed in an evacuated vacuum jar or sealed in a borehole package to reduce the effects of changes in barometric pressure and to provide additional thermal insulation. Shielding made of alloys with high magnetic permeability is placed around the sensor package to reduce electromagnetic interference. Finally, that part of the data acquisition system requiring operator interaction is located away from the vault or the wellhead containing

**Table 1.** Channels, Sensors, and Sections

Channel Name	Sample Rate	Sensor	Section Length, hours	Section Overlap, %
BH*00	20	STS-1, KS54000, or KS36000	1	0
LH*00	1	derived from BH*00	2–11	50
VH*00	0.1	derived from BH*00	24	50
BH*10	40	STS-2 or CMG-3	1	0
SH*10	40	GS13 or GS21	1	0

the sensors so that these sensors are disturbed as infrequently as possible. The calibration of the seismometers relies on the manufacturers' data for the absolute conversion factor between input ground motion and output voltage but the frequency response is measured periodically in situ.

[9] The staff of the IRIS Data Management Center (DMC) maintains an archive of all GSN data as well as a suite of software to extract data from the archive, reformat them into other common formats for analysis, and distribute the data to the research community. It also provides to users all metadata related to the sensor recordings, including information about instrument response. Both network operators periodically update detailed databases of response information, which are distributed to users by the IRIS DMC.

## 2. Analysis Methods

[10] For each station we processed the 20 sps data streams from the three orthogonal spatial components of the principal sensor (either an STS-1, KS-54000, or a KS36000) and the 1sps and 0.1 sps streams derived from them. In the broadly adopted FDSN SEED nomenclature, these were the BH\*-00, LH\*-00 and VH\*-00 channels, where the asterisk symbolizes any of three orientations. At those stations where data from auxiliary sensors (STS-2, CMG-3T, GS-13 or GS21) were also available, we also processed the 40 sps (BH\*-10 or SH\*-10) channels. Thus we examined 12 channels per station for those equipped with a separate sensor for short-period recording or 9 channels per station otherwise. Altogether, we processed more than 1 Tbyte of waveform data.

[11] We divided the year of data from each station-channel into nonoverlapping sections for BH\*-00 and BH\*-10 and 50% overlapping sections for LH\*-00 and VH\*-00, with the section lengths given in the Table 1. If less than 90% of the data for a particular segment was available we dropped that segment from the study.

[12] We computed a spectral estimate for each segment in identical fashion using the following steps: (1) removing the mean and trend from the time series, (2) applying a Hanning window to reduce spectral leakage, (3) computing a Fourier transform, and (4) removing the instrument response to obtain physical units. In a final step, we applied 1/7 decade bandwidth (approximately one-half octave), Gaussian filters to the Fourier transform to reduce the variance of the spectral estimates. The upper, central (geometric mean), and lower periods of each band are given by

$$P_u = 10^{(4-n)/14},$$

$$P_c = 10^{4-(n-1)/14},$$

$$P_l = 10^{4-(n-2)/14},$$

where  $n$  is the band number, with  $n = 1$  having a central period of 10,000 s. Thus for each band, the fractional bandwidth is

$$\frac{\Delta P}{P_c} = \frac{\Delta f}{f_c} = 10^{1/14} - 10^{-1/14} = 0.3304,$$

and each band overlaps its neighbor by 50%. The Gaussian filtered Fourier transform is given by

$$\overline{\text{FFT}}(f_c) = \int_{f_c - \Delta f}^{f_c + \Delta f} \text{FT}(f) e^{-f^2/2} df \bigg/ \int_{f_c - \Delta f}^{f_c + \Delta f} e^{-f^2/2} df,$$

where FT is the unfiltered Fourier transform.

[13] As we processed each station-channel, we plotted the spectral estimates as a function of time for each band to assess the data quality. In Figure 2 we show an example of such a single plot in this case of the BHZ-00 channel for station CASY. The anomalous spectral estimates between samples 3500 and 4000 are indicative of instrumental problems, most likely caused by a "dead" channel. In a case such as this, we dropped data from the affected period from the analysis.

[14] The end product of the above procedures is a data set of over 738,000 spectral estimates. To illustrate, we plot all observations for a single station-channel band as a function of time in Figure 3, in this case the VHZ-00 channel (vertical component STS-1) of station TUC (Tucson, Arizona) for a single period, 316 s. The top panel shows spectral estimates as a function of time (24 hour long, 50% overlapping samples). The prominent spikes represent energy arriving at the station from earthquakes; no effort was made to exclude earthquake signals from the data set. Overall, the noise background varies as weather and other factors contribute but the performance of this station is uniformly good throughout the entire year.

[15] In the middle panel, we plot the distribution of these estimates as percentiles and from this we save the 1st, 5th, 25th, and 50th percentiles for comparison with similar measurements from other stations. Most of the estimates in this subset fall below  $-185$  dB, making TUC a very quiet station in this band. Fewer than 7% of the observations fall in the range  $-160$  to  $-80$  dB where seismic signals dominate. For a quiet station like TUC, there is only a small difference between the 1st and 5th percentiles at the quiet end of the distribution. The behavior of the upper end

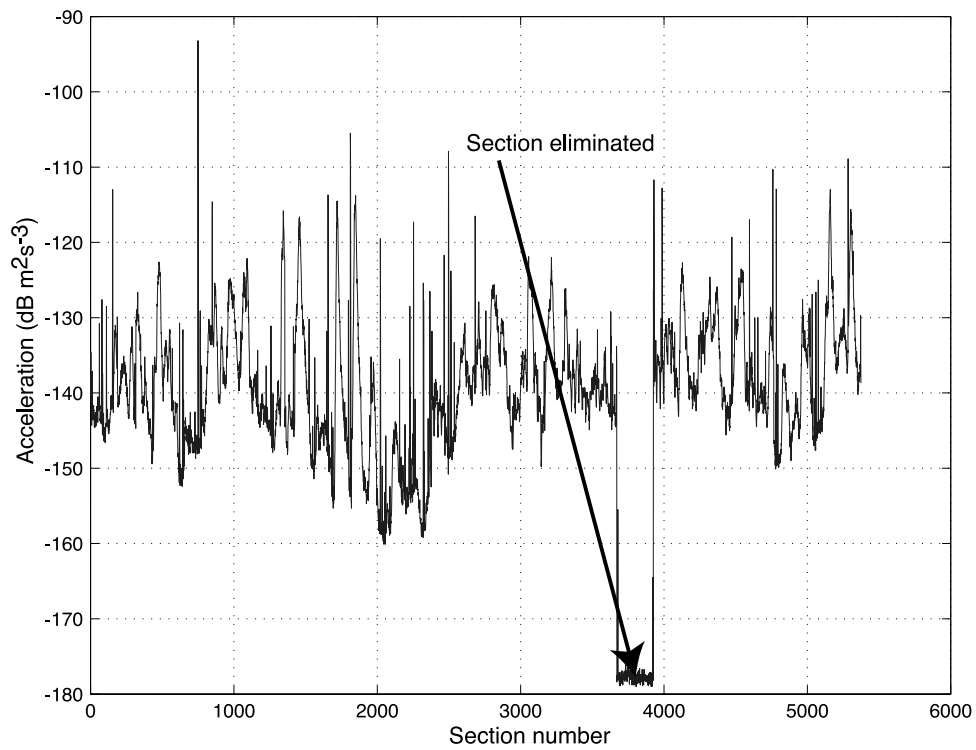


**Figure 2.** Variation of background noise for CASY-BHZ00 in period band 316 s as a function of time. Each section represents a 50% overlapping 2 hour average. In this instance an instrument failure caused anomalous results in the section indicated, and consequently, that portion of this set was eliminated from further analysis.

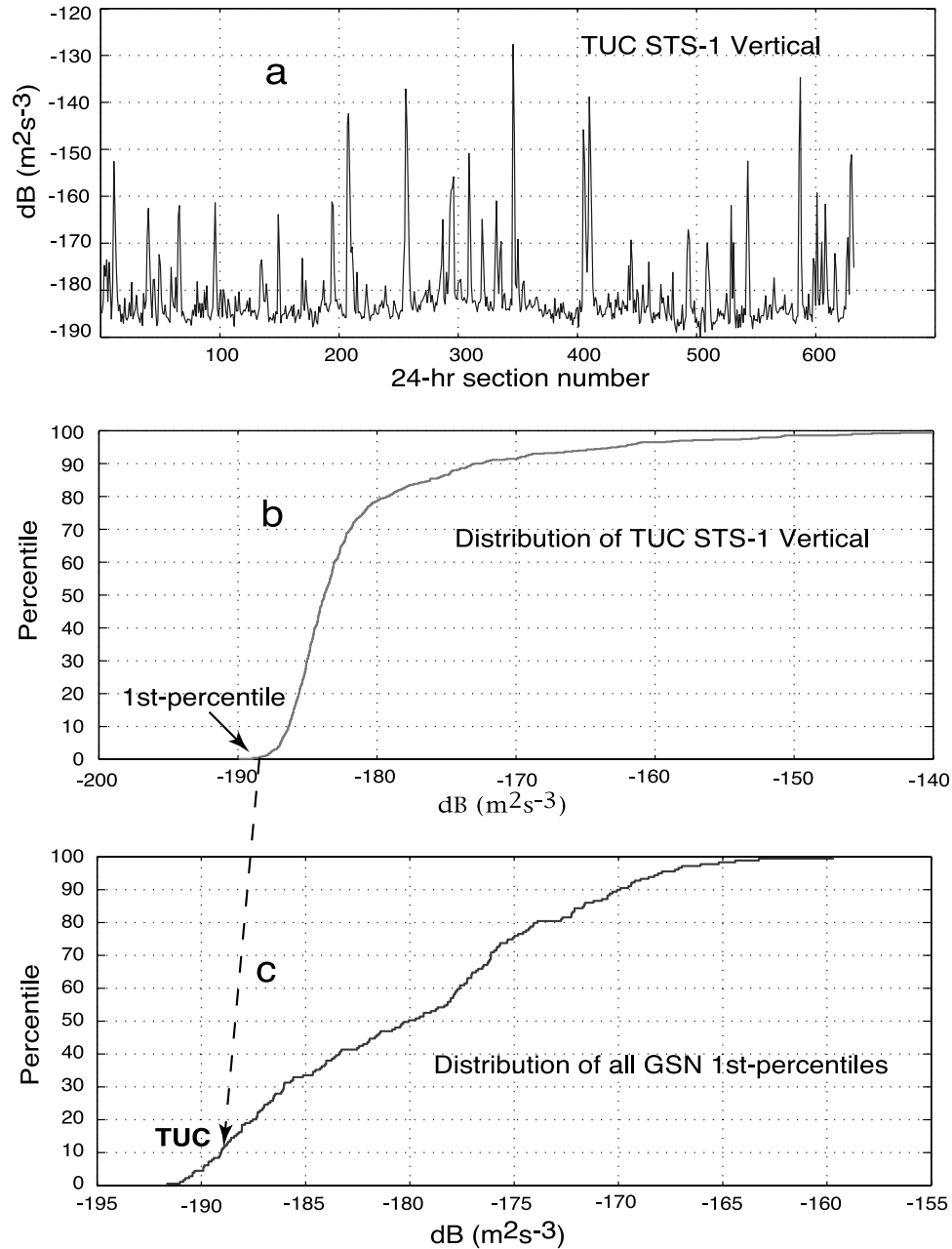


**Figure 3.** Illustrative results for the band centered at 316 s. (a) Variation of background noise for a single station-channel (TUC-VHZ00) in the period band over the year analyzed. (b) Distribution of noise estimates for background noise for TUC-VHZ00 in the band. (c) Distribution of 1st-percentile estimates from all GSN vertical component channels in the band.

**Table 2.** The GSN Noise Model<sup>a</sup>

Period	Min H	Min Z	Period	Min H	Min Z
10000.000	-143.9	-153.8	22.758	-179.4	-178.9
8483.429	-145.5	-155.7	19.307	-175.1	-173.7
7196.857	-148.0	-160.8	16.379	-172.5	-168.3
6105.402	-150.3	-164.0	13.895	-168.0	-166.0
5179.475	-151.7	-167.2	11.788	-169.5	-167.8
4393.971	-152.3	-168.7	10.000	-169.3	-164.8
3727.594	-152.2	-171.5	8.483	-162.4	-156.2
3162.278	-154.3	-173.2	7.197	-155.1	-148.9
2682.696	-155.5	-174.5	6.105	-152.4	-146.2
2275.846	-156.9	-176.5	5.179	-147.8	-141.5
1930.698	-158.0	-177.5	4.394	-144.9	-139.0
1637.894	-159.3	-178.1	3.728	-146.7	-140.7
1389.495	-161.0	-180.4	3.162	-148.6	-144.2
1178.769	-163.9	-181.4	2.683	-151.0	-146.8
1000.000	-167.1	-183.0	2.276	-154.3	-149.7
848.343	-168.8	-183.7	1.931	-157.0	-152.4
719.686	-171.2	-185.4	1.638	-159.7	-155.6
610.540	-173.2	-186.7	1.389	-163.0	-158.6
517.948	-175.8	-188.6	1.179	-165.5	-160.9
439.397	-176.7	-189.7	1.000	-168.5	-163.4
372.759	-178.4	-190.8	0.848	-171.3	-165.2
316.228	-180.6	-191.6	0.720	-171.5	-167.6
268.270	-182.5	-191.0	0.611	-170.5	-167.2
227.585	-183.5	-190.1	0.518	-169.0	-166.8
193.070	-183.6	-188.6	0.439	-167.8	-166.6
163.789	-183.3	-187.8	0.373	-165.8	-166.4
138.950	-184.2	-187.6	0.316	-164.6	-166.6
117.877	-184.6	-187.3	0.268	-164.1	-166.0
100.000	-184.3	-188.2	0.228	-163.2	-165.4
84.834	-184.6	-188.9	0.193	-161.9	-164.2
71.969	-185.8	-189.5	0.164	-161.9	-162.1
61.054	-187.0	-189.7	0.139	-161.2	-161.5
51.795	-187.1	-189.3	0.118	-159.6	-162.3
43.940	-186.9	-188.8	0.100	-159.2	-160.7
37.276	-185.6	-187.7	0.085	-159.2	-159.3
31.623	-184.8	-186.4	0.072	-162.4	-160.6
26.827	-183.1	-183.9			

<sup>a</sup>At each period we list the horizontal (Min H) and vertical (Min Z) component 1st percentile acceleration in dB relative to  $1 \text{ m}^2 \text{ s}^{-3}$ .

of the distribution might depend on a station's proximity to seismogenic zones and was not examined in this study.

[16] In the bottom panel of Figure 3, to get an idea of how well the overall network performs, we have plotted all 1st-percentile estimates from the vertical components of all stations of the GSN in this set. That is, we choose from each station-channel a single number representing the 1st-percentile of its distribution. From this type of plot we can evaluate how well an individual station compares with the network.

[17] For each station-channel subset of spectral estimates, we calculate the 1st, 5th, 25th, and 50th percentile values of that distribution and tabulate them as a function of period (see auxiliary material)<sup>1</sup>. We then group these values with similarly determined values for all station-channel subsets in the total data set. In Table 2 we list the minimum values for the 1st percentile observations as a function of period, and in Figure 4 we plot the minimum values at each period for these four percentiles. For ease of comparison, the PLNM is included in the plot.

[18] For those periods where there are multiple channel subsets for a single component (BHZ00, BHZ10 and LHZ00 at 100 s, for example) we choose the minimum estimate to represent that station, and then examine the

distribution of observations for all stations. The 1st percentile estimates for the network are plotted in Figures 5–7. Each rectangle in these figures is 1 dB in height, 1/14 of a decade in width (so as not to overlap its neighbor) and is colored according to the number of stations whose spectral estimates lie in that range of period and spectral level. The envelope of the minima forms the GSN Noise Model. Also shown in Figure 5 and 6, for comparison, is the PLNM.

[19] In a separate analysis of the VHZ channels intended to resolve the fundamental mode peaks in the background spectra [*Suda et al.*, 1998], we increased the frequency resolution by omitting the step in which the 1/7 decade Gaussian filters were applied. We then preselected the quietest data by choosing those observations whose mean square noise averaged over the band 2 to 7 mHz was no greater than 4 times the minimum level. In Figure 8 we show the results of a stack of this subset for the 32 quietest stations. The bandwidth is  $1.16 \times 10^{-5}$  Hz. As many other investigators have observed, the fundamental mode peaks stand out well while the background noise is suppressed by the stacking process. The reduction in the variance of the spectrum for periods shorter than 200 s may be due to averaging of many different Rayleigh wave paths on a heterogeneous Earth.

[20] Finally, in Figure 9 we show the minimum 1st-percentile noise estimates for all GSN channels separated by sensor type. Those stations equipped with the STS-1 sensor clearly show much lower noise for periods longer than 100 s than stations equipped with the other types of sensors. For periods longer than 100 s the noise observed at stations equipped with the CMG-3T sensor is similar to the levels observed with the STS-2 or CMG-3TB sensor.

### 3. Discussion

[21] Over most of the bandwidth covered by the GSN, the 1st-percentile spectral values are lower than those of the PLNM. The exception to this is for periods less than about 0.4 s. Here the minimum spectral values of the GSN Noise Model are significantly higher than those for the PLNM. It is worth noting in this regard that the PLNM at short periods was determined by just a few stations that were equipped with short-period borehole seismometers optimized for small-signal detection (RSNT equipped with a S750 in a 100m borehole, Alice Springs and BOSA equipped with borehole GS21s). As *Peterson* [1993] noted in his analysis, there was inadequate data to determine the noise for periods shorter than 0.5 s; the data set from the latter two stations consisted of a single 4096-sample section.

[22] All minimum noise levels, both horizontal and vertical, are observed on STS-1 seismometers for periods longer than 1.4 s. At periods longer than about 120 s, the observed vertical component minimum noise levels are lower than the theoretical KS54000 seismometer instrument noise. At periods longer than about 300 s, the observed vertical component noise levels are close to the theoretical STS-1 seismometer noise [*Wielandt*, 2002]. Lower noise levels have been observed by superconducting gravimeters for periods longer than about 1000 s [*Rosat et al.*, 2003]. At least some of the very long-period vertical noise is caused by local fluctuations in atmospheric pressure [*Zurn and Widmer*, 1995; *Beauduin et al.*, 1996].

<sup>1</sup>Auxiliary material is available at <ftp://ftp.agu.org/apend/jb/2004JB003408>.

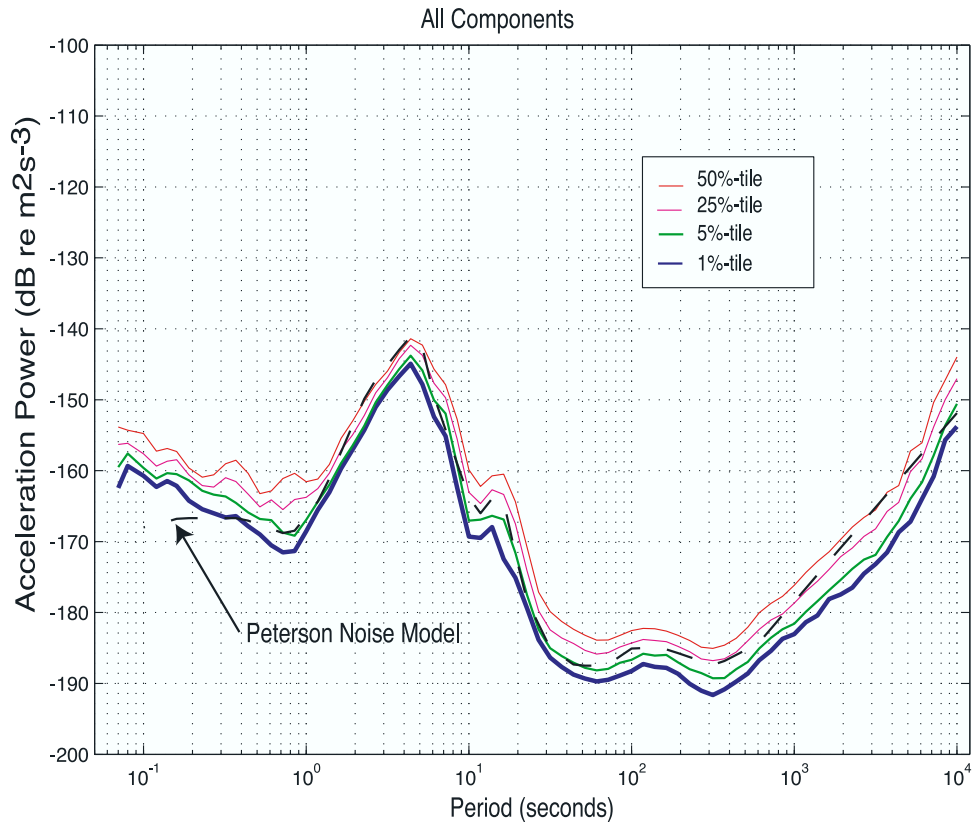


**Figure 4.** Minimum noise levels at the 1st, 5th, 25th, and 50th percentiles for all stations and channels with the PLNM for comparison.

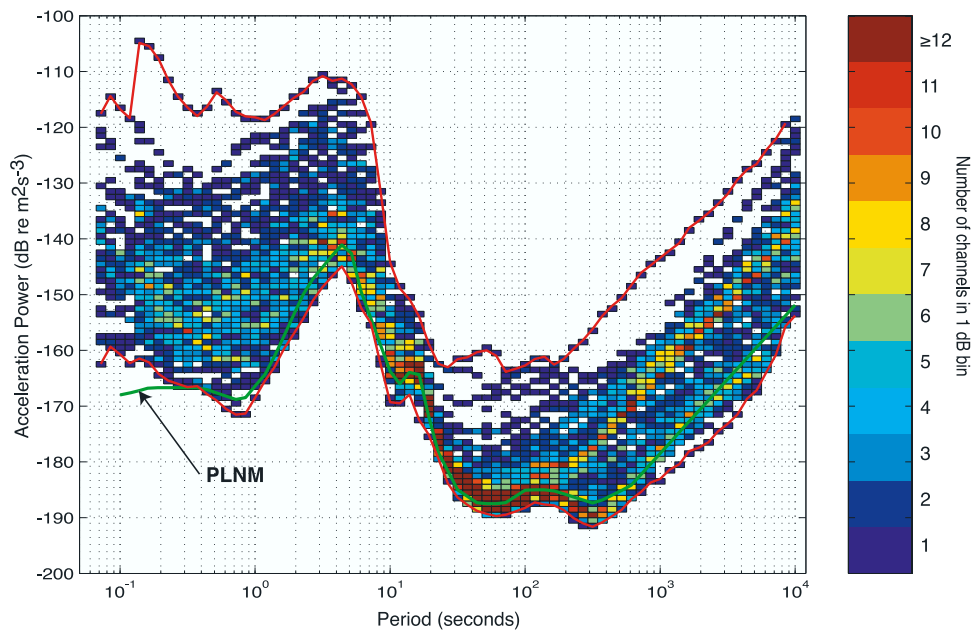


**Figure 5.** Results found by computing density of observations, one per component per station, for all 118 stations considered in this study. The colors indicate how many stations' spectral estimates lie in each 1 dB by 1/14th decade rectangle. This plot includes contributions from both horizontal and vertical channels.

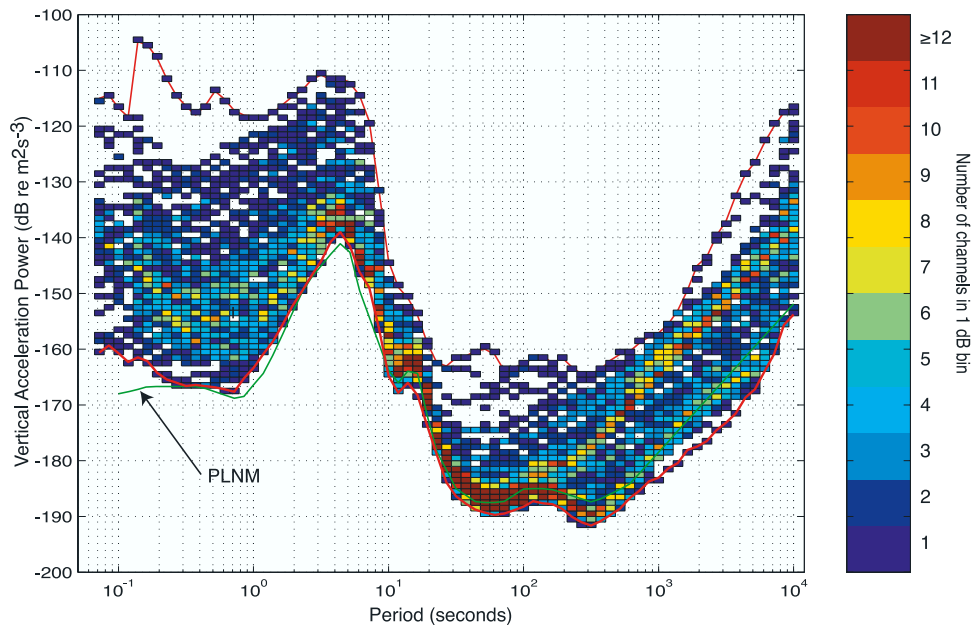


**Figure 6.** Results found by computing density of observations, vertical component only, for all 118 stations considered in this study. The colors indicate how many stations' spectral estimates lie in each 1 dB by 1/14th decade rectangle.

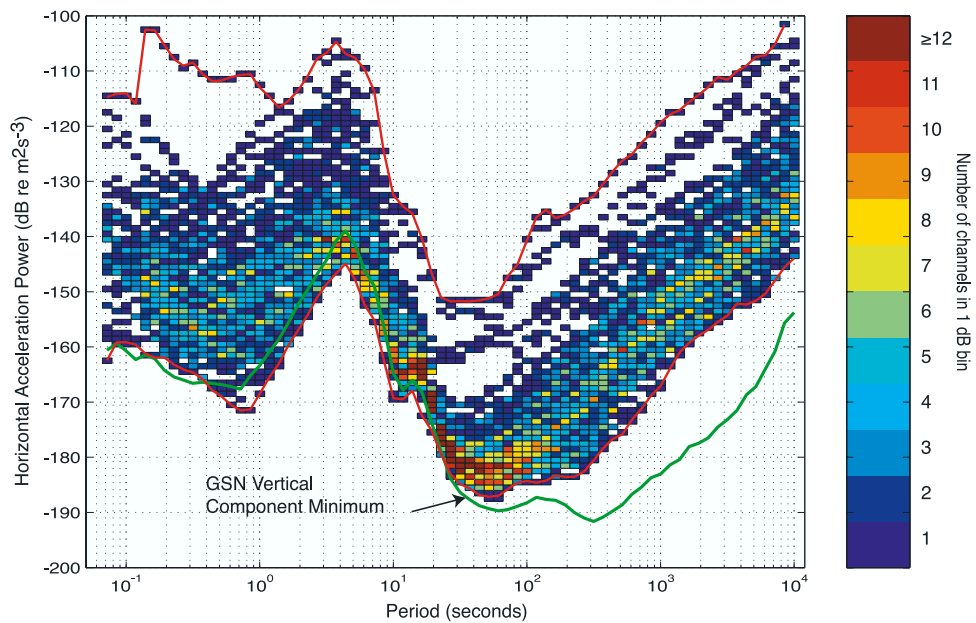


**Figure 7.** Results found by computing density of observations, horizontal component only, for all 118 stations considered in this study. The colors indicate how many stations' spectral estimates lie in each 1 dB by 1/14th decade rectangle.

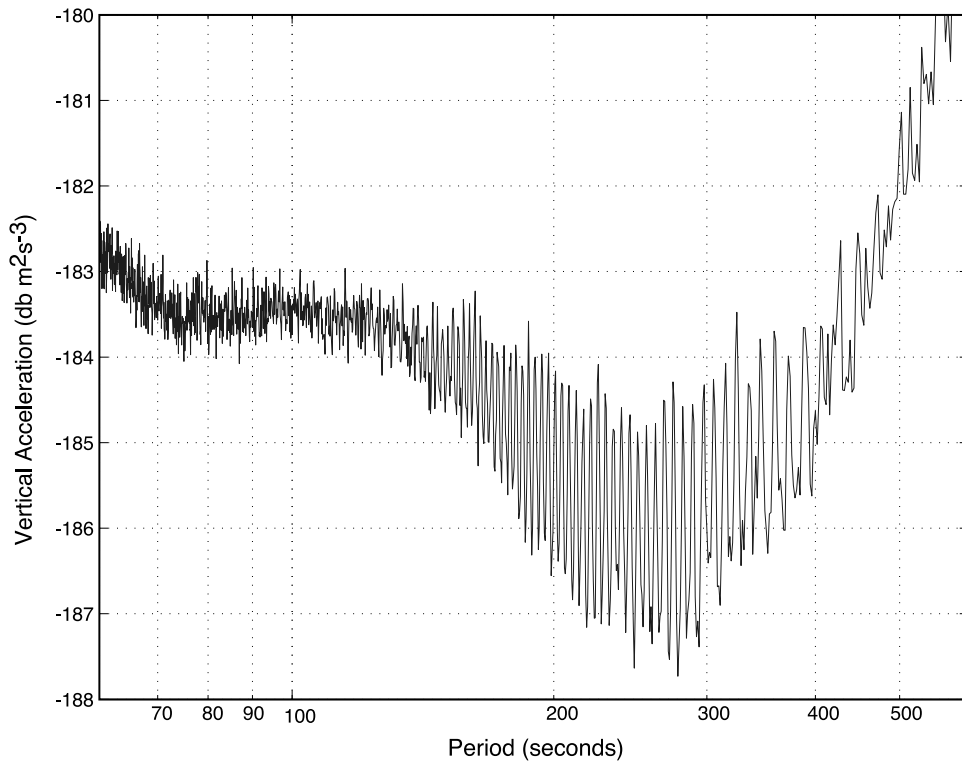


**Figure 8.** A stack of the raw spectra of the quietest 32 vertical channels. The bandwidth of these estimates is  $1.16 \times 10^{-5}$  Hz.

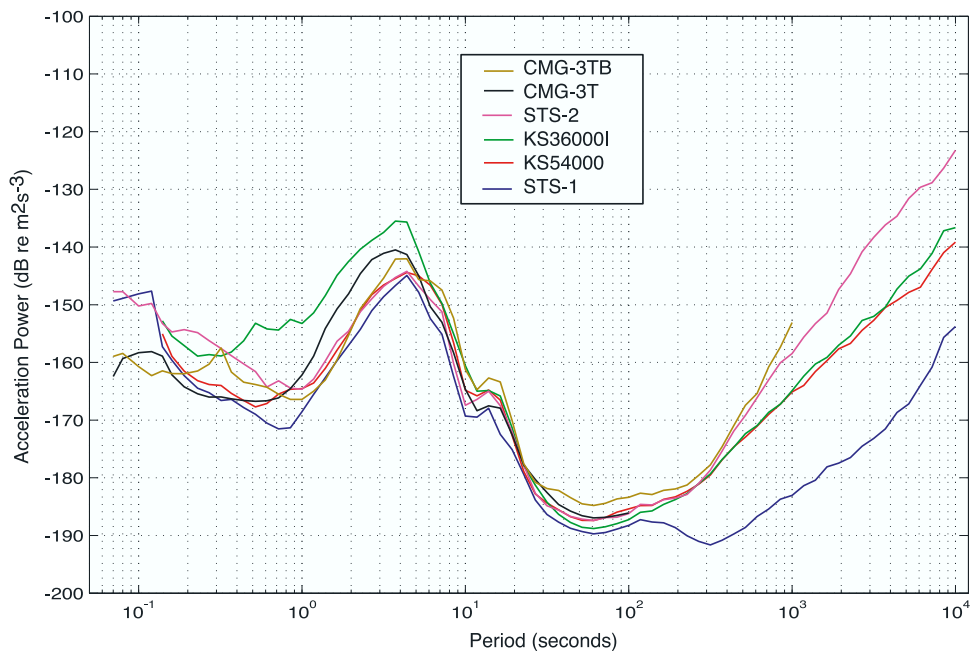


**Figure 9.** GSN 1st-percentile noise plotted by sensor.

[23] The minimum horizontal component noise levels are less than the vertical component noise levels through the microseism band but considerably higher for periods longer than about 30 s. There is no systematic bias between the levels of the two directions of horizontal noise. At long periods, some of the horizontal component noise may be caused by local atmospheric pressure fluctuations [Beauduin *et al.*, 1996] but a more likely source is thermally induced tilts. The lowest horizontal component noise levels are observed at stations where the seismometers (all STS-1) are located in tunnels or very well insulated vaults.

[24] The shape of the GSN Noise Model spectrum in the normal mode band is controlled by the ‘tail’ of the microseismic noise decreasing toward longer periods and the general increase in noise toward yet longer periods, with a ‘hump’ in between. This hump, which is a global feature (also discernable in the PLNM), is likely a reflection of the persistent excitation of the fundamental normal modes [Suda *et al.*, 1998]. Infragravity waves in the ocean provide an energetic source peaked at around 100 s [Webb, 1998], which can provide continuous excitation of these fundamental normal modes [Rhie and Romanowicz, 2004].

[25] **Acknowledgments.** Global Seismographic Network (GSN) is a cooperative scientific facility operated jointly by the Incorporated Research Institutions for Seismology (IRIS), the United States Geological Survey (USGS), and the National Science Foundation (NSF). The GSN is maintained by two operational groups: the USGS Albuquerque Seismological Laboratory (ASL) in Albuquerque, NM, and Project IDA of the University of California San Diego. The facilities of the IRIS Data Management System, and specifically the IRIS Data Management Center, were used for access to waveform and metadata and for calculating the spectral estimates. We would like to thank the staff of the IRIS DMC, and particularly Rick Benson, Anh Ngo, and Mary Edmunds, for their assistance in processing this massive data set. We also thank Bob Hutt and Harold Bolton of the USGS for their helpful discussions. The IRIS GSN and DMS are funded through the National Science Foundation and specifically the GEO Directorate through the Instrumentation and Facilities Program of the National Science Foundation under Cooperative Agreement EAR-0004370.

## References

Agnew, D. C., and J. Berger (1978), Vertical seismic noise at very low frequencies, *J. Geophys. Res.*, *83*, 5420–5424.

- Ahern, T. K., R. Buland, and S. Halbert (1994), SEED format version 2.3 reference manual, report, Inc. Res. Inst. for Seismol., Washington, D. C.
- Beauduin, R., P. Lognonne, J. P. Montagner, S. Cacho, J. F. Karczewski, and J. Morand (1996), The effects of the atmospheric pressure changes on seismic signals or how to improve the quality of a station, *Bull. Seismol. Soc. Am.*, *86*, 1760–1769.
- Brune, J. N., and J. Oliver (1959), The seismic noise of the Earth’s surface, *Bull. Seismol. Soc. Am.*, *49*, 349–353.
- Butler, R., et al. (2004), The Global Seismographic Network surpasses its design goal, *Eos Trans. AGU*, *83*, 23.
- Fix, J. E. (1972), Ambient Earth motion in the period range from 0.1 to 2560 sec, *Bull. Seismol. Soc. Am.*, *62*, 1753–1760.
- Frantii, G. E., D. E. Willis, and J. T. Wilson (1962), The spectrum of Earth noise, *Bull. Seismol. Soc. Am.*, *52*, 113–121.
- Incorporated Research Institutions for Seismology (1994), *Federation of Digital Seismographic Networks Station Book*, IRIS Data Manage. Cent., Seattle, Wash.
- Murphy, A. J., and J. R. Savino (1975), A comprehensive study of long-period (20–200s) Earth noise at the high gain worldwide seismograph stations, *Bull. Seismol. Soc. Am.*, *65*, 1827–1862.
- Peterson, J. (1980), Preliminary observations of noise spectra at the SRO and ASRO stations, *U.S. Geol. Surv. Open File Rep.*, 80-99.
- Peterson, J. (1993), Observations and modeling of seismic background noise, *U.S. Geol. Surv. Open File Report*, 93-322.
- Rhie, J., and B. Romanowicz (2004), Excitations of the Earth’s incessant free oscillation by atmosphere-ocean-seafloor coupling, *Nature*, *431*, 552–556.
- Rosat, S., J. Hinderer, D. Crossley, and L. Rivera (2003), The search for the Slichter mode: Comparison of noise levels of superconducting gravimeters and investigation of a stacking method, *Phys. Earth Planet. Inter.*, *140*, 183–202.
- Suda, N., K. Nawa, and Y. Fukao (1998), Earth’s background free oscillations, *Science*, *279*, 2089–2091.
- Webb, S. C. (1998), Broadband seismology and noise under the ocean, *Rev. Geophys.*, *36*, 105–142.
- Wielandt, E. (2002), Seismometry, in *International Handbook of Earthquake & Engineering Seismology, Part A*, edited by W. H. K. Lee et al., pp. 283–304, Academic, San Diego, Calif.
- Zurn, W., and R. Widmer (1995), On noise reduction in vertical seismic records below 2 mHz using local barometric pressure, *Geophys. Res. Lett.*, *22*, 3527–3540.

J. Berger and P. Davis, Institute of Geophysics and Planetary Physics, Scripps Institution of Oceanography, University of California San Diego, 9500 Gilman Drive, La Jolla, CA 92093-0225, USA. (jberger@ucsd.edu; pdavis@ucsd.edu)

G. Ekström, Department of Earth and Planetary Sciences, Harvard University, 20 Oxford Street, Cambridge, MA 02138, USA. (ekstrom@seismology.harvard.edu)